GEOCHEMISTRY, MINERALOGY AND PETROLOGY • SOFIA
ГЕОХИМИЯ, МИНЕРАЛОГИЯ И ПЕТРОЛОГИЯ • СОФИЯ
2008, **46**, 69-84.

Mineralogy of diopside-phlogopite marbles from the Modi-Khola valley, the Central Nepal Himalaya

Rossitsa D. Vassileva, Ivan K. Bonev

Abstract. The diopside-phlogopite marbles, found in the valley of Modi-Khola river, belong to the informal Unit II of the metamorphic Greater Himalayan sequence. Major diopside, phlogopite and scapolite associate with retrograde actinolite, titanite, troilite and tourmaline. Two chemical types of diopside are assigned: 1. ferroan-diopside with 8.36-9.94 wt.% FeO, 11.39-12.47 wt.% MgO, and $Mg/(Mg+Fe^{2+})$ ratio 0.69, presented by green prismatic and irregular crystals and grains; 2. diopside with 2.69-5.74 wt.% FeO, 14.92-20.38 wt.% MgO, $Mg/(Mg+Fe^{2+})$ ratio 0.89, and white to colorless well shaped crystals. The diopside unit-cell parameters are: *a* 9.749(3); *b* 8.921(1); *c* 5.249(7) Å; *β* 105.836(8)°. Ca-scapolite with ~80 mol% Me is meionite member of the marrialite-meionite series, with *a* 12.181(1); *c* 7.571(7) Å. Ca-amphibole with ~16 wt.% MgO, ~13.4 wt.% FeO and $Mg/(Mg+Fe^{2+})$ ratio 0.69, equal with those of the replaced pyroxene, is determined as actinolite with *a* 9.843(7); *b* 18.049(4); *c* 5.285(8) Å; *β* 104.877(1)°. The mica presented is a Mg-member of the annite-phlogopite solid solution, belonging to the group of trioctahedral true micas with 16.50-24.01 wt.% MgO, ~ 9.68 wt.% K_2O, 7.46-10.46 wt.% FeO and up to 0.83 wt.% TiO_2. It is defined as ferroan-phlogopite with *a* 5.31(7); *b* 9.20(4); *c* 10.31(8) Å; *β* 99.9(1)°. Actinolite contains plenty of oriented diopside relics and is overgrown by phlogopite.

Key words: diopside, scapolite, phlogopite, actinolite, marble, Modi-Khola, Greater Himalaya

Address: Geological Institute, Bulgarian Academy of Sciences, 1113 Sofia, Bulgaria;
E-mail: rosivas@geology.bas.bg

Росица Д. Василева, Иван К. Бонев. Минералогия на диопсид-флогопитовите мрамори от долината на Моди-Кхола, Централни Непалски Хималаи

Резюме. Диопсид-флогопитовите мрамори от долината на река Моди-Кхола, принадлежат към неформалната Единица II от метаморфната последователност на Високите Хималаи. Основните минерали в калк-силикатните скали са диопсид, флогопит и скаполит, които тясно асоциират с ретроградна парагенеза от актинолит, титанит, троилит и турмалин. Определени са два типа диопсид според химизма: 1. Fe-съдържащ диопсид с 8,36-9,94 тегл.% FeO, 11,39-12,47 тегл.% MgO, $Mg/(Mg+Fe^{2+})$ 0,69, представен от зелени призматични и скелетни кристали и зърна; 2. диопсид, съдържащ 2,69-5,74 тегл.% FeO, 14,92-20,38 тегл.% MgO, и $Mg/(Mg+Fe^{2+})$ 0,89, с бели до безцветни добре оформени кристали. Параметрите на елементарната клетка на диопсида са: *a* 9,749(3); *b* 8,921(1); *c* 5,249(7) Å; *β* 105,836(8)°. Скаполит с ~80 мол% мейонитова молекула е определен като мейонит, калциев член на мариалит-мейонитовата изоморфна редица с *a* 12,181(1); *c* 7,571(7) Å. Калциев амфибол съдържащ ~16 wt.% MgO, ~13,4 wt.% FeO, и $Mg/(Mg+Fe^{2+})$ 0,69 е определен като актинолит с параметри на елементарната клетка *a* 9,843(7); *b* 18,04 9(4); *c* 5,285(8) Å; *β* 104,877° (1).

Слюдата е Mg-член на анит-флогопитовата изоморфна редица, от групата на триоктаедричните истински слюди с 16,50-24,01 тегл.% MgO, ~ 9,68 тегл.% K_2O, 7,46-10,46 тегл.% FeO и до 0,83 тегл.% TiO_2. Определя се като Fe-съдържащ флогопит с *a* 5,31(7); *b* 9,20(4); *c* 10,31(8) Å; *β* 99,9(1)°. Актинолитът съдържа обилни ориентирани реликти от диопсид и е последващо обраснат от флогопит.

Introduction

The Himalayas – the higher mountain system in the world, stretching over 2400 km, are a result of complex geological processes of sedimentation, metamorphism, granitization, magmatism and intensive tectonic movements. The geology of the Himalaya is a record of the most dramatic and visible creations of the modern plate tectonic forces. This huge mountain range is a result of the collision of two continental plates – Indian and Eurasian in Eocene (c. 50 Ma) and convergence, deformation and uplift has continued to present day.

The calc-silicate rocks, developed in the region southwards of the Annapurna range are a specific rock type in the valley of the Modi-Khola River, near the Hinko cave. The diopside and phlogopite marbles are formed by prograde regional metamorphic processes. They are subsequently cross-cut by pegmatite veins, which led to recrystallization with the formation of lenses with larger silicate crystals. A strong retrogressive phase with a fluid composition rich in H_2O is documented by the growth of actinolite and titanite and later hydrothermal minerals.

The purpose of this paper is to describe the mineral composition of the diopside marbles, part of the Greater Himalayan sequence, exposed in the valley of the Modi-Khola river. Emphasis is placed on physical and chemical characteristics of the silicate minerals and on the relationships between the minerals in the process of formation.

Geological setting

The Modi-Khola valley is located in central Nepal and cuts from south to north through three distinct tectonostratigraphic units of the central Himalayan orogen (Fig. 1):

1. The Lesser Himalayan sedimentary sequence, composed by Precambrian to Mesozoic low-grade metasediments (Dhital et al. 2002).

2. The metamorphic core of the Himalayan orogen, namely the Greater Himalayan metamorphic sequence is composed of kyanite- and sillimanite-grade gneisses, intruded by variably deformed Miocene leucogranites (Godin 2003). The rocks of the Greater Himalayan sequence are widely exposed, being the highest-grade rocks in the Himalaya with termobarometric conditions of formation ~10-14 kbar and 700-800°C (Ganguly et al. 2000; Stephenson et al. 2000; Kohn et al. 2004). In central Nepal, Greater Himalayan sequence is informally subdivided into three formations (Bordet et al. 1971; Le Fort 1975, 1981; Colchen et al. 1986; Pêcher 1989; Guillot et al. 1995). The rocks of these three formations are highly deformed and have been a subject to regional metamorphism, sometimes intercalated with other lithologies. Searle & Godin (2003) proposed the use of more general "units", rather than "formation". Unit I is the lowest in structural respect, pellitic, consisting of schists and gneisses formed by metamorphism of sedimentary succession, dominated by mudstones and interbedded minor sandstones. Unit II is dominantly calc-silicate and consists of marbles and layered calc-silicate schist and calc-silicate gneisses. This formation sits structurally above Unit I. Certain K-feldspar augen gneisses known as granitic Unit III intrude near the structural top of Unit II.

3. The Tethyan sedimentary sequence, compiled by a nearly continuous 10-km thick succession of Neoproterozoic to Eocene sedimentary rocks that extend from the South Tibetan Detachment System north to the Indus–Yarlung suture zone, which marks the former subduction zone between the Indian and Eurasian plates (Bordet et al. 1971; Colchen et al. 1986; Garzanti 1999; Murphy & Yin 2003). Lowermost Tethyan strata may be the protoliths for Greater Himalayan metasedimentary

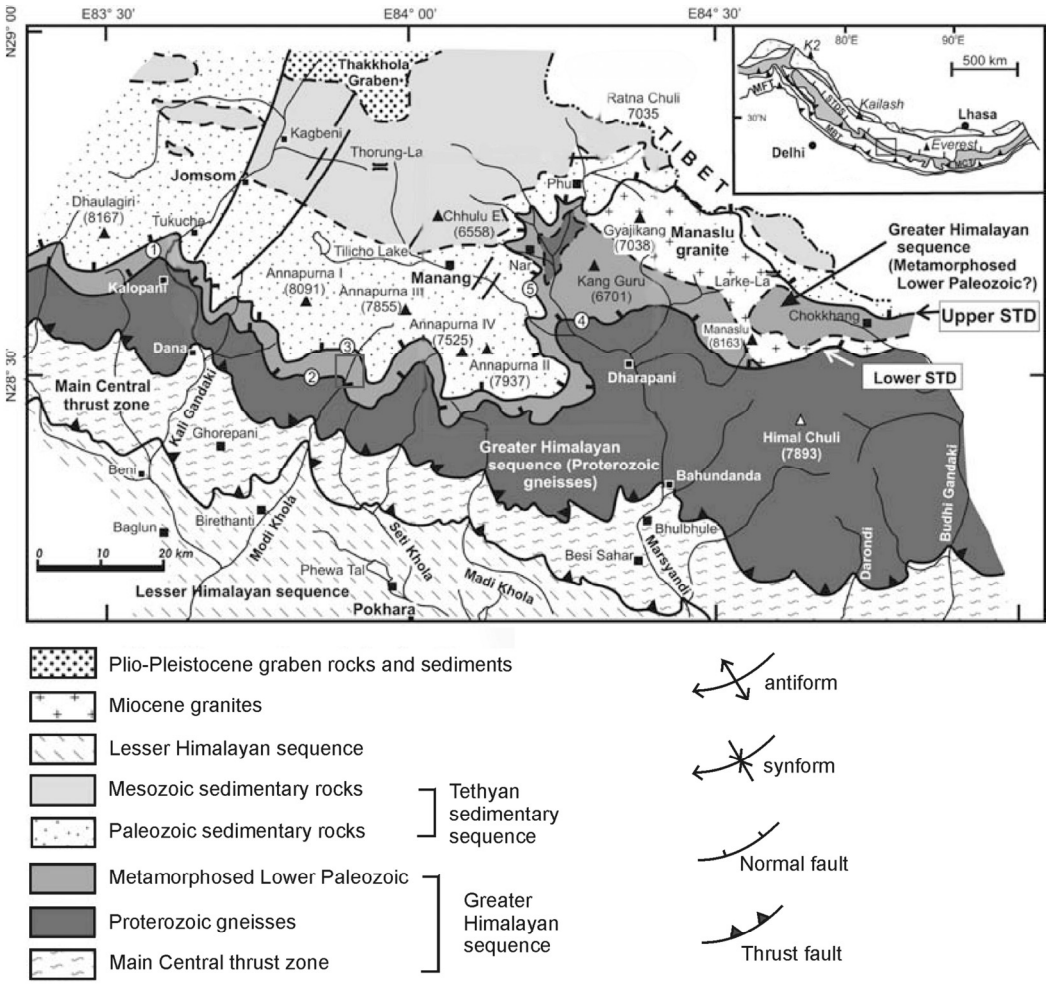

Fig. 1. Regional geological map modified after Godin et al. (2006). Greater Himalayan sequence in grey; Unit I proterozoic gneisses in dark gray and Unit II calc-silicate rocks in light gray. Solid rectangle refers to the studied area. The numbers indicate the various strands of the South Tibetan detachment system: (1) Annapurna detachment; (2) Deurali detachment; (3) Machapuchare detachment; (4) Chame detachment; (5) Phu detachment

rocks (Myrow et al. 2003; Richards et al. 2005).

The three tectonostratigrafic units are separated by two major north-dipping tectonic boundaries that were active during the Miocene: the Main Central Thrust and the South Tibetan Detachment system (Godin 2003; Searle et al. 2003). The Main Central Thrust (Le Fort 1975; Colchen et al. 1986; Pêcher 1989) is the structure that bounds the base of the Greater Himalayan series. It places higher-grade Greater Himalayan metasedimentary rocks on lower-grade Lesser Himalayan metasedimentary rocks. Lately, the Main Central Thrust is described as a complex high-strain shear zone affecting both the upper part of the Lesser Himalayan sediments and the lower section of the Greater Himalayan

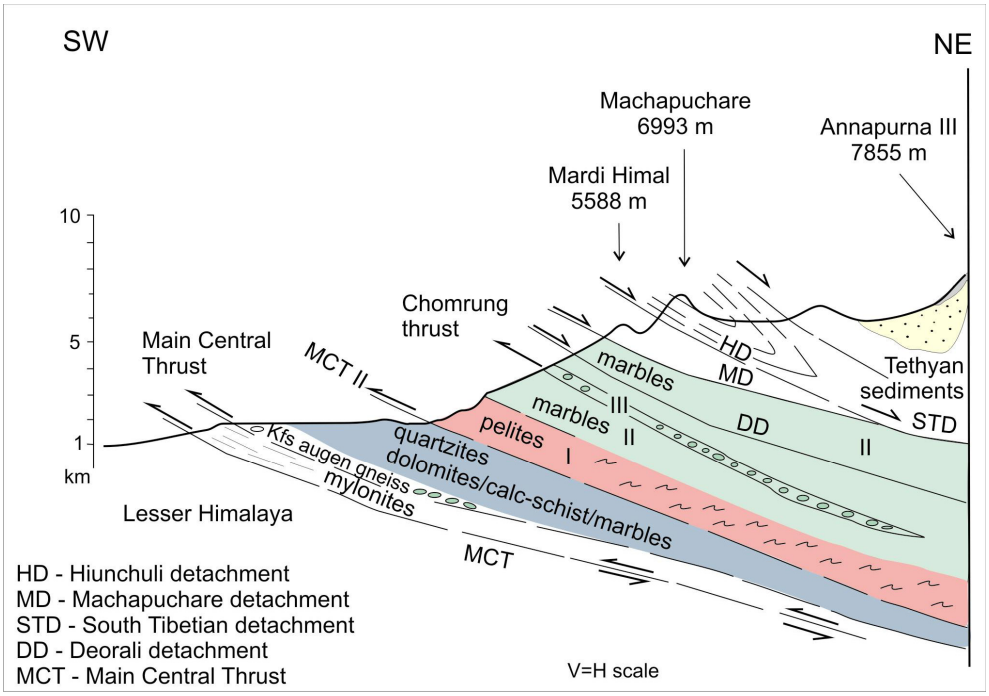

Fig. 2. Section along the Modi-Khola river, modified after Hodges et al. (1996) and Searle & Godin (2003). I, II, III refer to the informal units of the Greater Himalayan metamorphic sequence

metamorphites (Stephenson et al. 2000) with very recent motion in Late Miocene-Pliocene (Kohn et al. 2001). The South Tibetan Detachment System marks the top of the Greater Himalayan series, and consist of north-dipping normal faults (Searle et al. 2003). Initial works failed to recognize it and interpreted the Tethyan sediments as stratigrafically overlaying the high-grade rocks of the Greather Himalayan sequence. The South Tibetan Detachment system places less-metamorphosed Tethyan series metasedimentary rocks on more-metamorphosed Greater Himalayan series metasedimentary rocks.

The huge glacier circus bordered by the range of Annapurna peaks, known as Annapurna Sanctuary follows the general E-W orientation of the tectonic boundaries. The valley of the Modi-Khola river cross-cuts the range in a meridional direction, forming deep section through the mountain. The peaks of South Annapurna and Hiunchuli raise over the western banks, while the spectacular sharp tooth of Machapuchare stands eastwards.

The valley of Modi-Khola is a section through the rocks of the Greater Himalayan sequence (Fig. 2). In the lower parts of the section the pellitic rocks of Unit I are seen, presented by gneisses and schists. Kyanite impregnations are often observed. In lower parts the gneisses are garnet-bearing. The calc-silicate rocks from Unit II are well exposed and prevail in the middle part of the Modi-Khola valley. Marbles and layered calc-silicate schists and gneisses, together with pegmatite veins are the main lithologies. The marble horizons show massive and granular texture, but very often they are fine-layered. Relatively pure marbles alternate with layered marbles containing inclusions of diopside and phlogopite in different ratios. Silicates could be found together or separately. Phlogopite marbles

show clear cleavage in accordance with the equal orientation of the mica crystals in the fine layers. Diopside in some marble horizons forms monomineral concentrations and lenses, sometimes up to 10 cm, arranged following the general orientation of the marble strata.

Pegmatites are vastly spread among the calc-silicate rocks in the middle parts of the section through Modi-Khola valley. They are closely interacting with the embedding marbles. Two genetically different pegmatite types can be separated. Often in the central parts of the pegmatite bodies pyrite altered to limonite is observed.

Type I pegmatites are fine- and equi-granular, showing shistosity parallel to the calc-silicate layers. Tourmaline needle-like crystals are often observed.

Type II pegmatites are coarse-grained, with larger up to several cm crystals of composing quartz, K-feldspar and mica. These veins clearly cross-cut the Type I pegmatites, and the marble layers. Tourmaline is abundant accessory mineral, forming up to several cm zone at the crossings with Type I pegmatites and gneisses.

At the contacts with the marbles the diopside quantity increases in accordance with the increased size of the single crystals. In the central zones near the pegmatites the diopside crystals reach up to 10 cm in length.

The widespread in the Modi-Khola valley diopside and phlogopite marbles are products of the regional metamorphism, but in the space around the pegmatite bodies, especially of Type II, processes of recrystallization occur.

Methods

Mineral relationships, paragenetic sequences, some physical and optical constants of the minerals were determined by macroscopic observations and especially by microscopic studies using transmitted light polarising microscope. Selective dissolution (with 5% HCl) of the carbonate matrix in several samples gave an opportunity for extraction of the individual crystals and their aggregates, thus making them accessible for direct observation. Morphology of the single crystals was studied by SEM on carbon-coated samples. Chemical analyses were performed by electron probe microanalyser JEOL Superprobe 733 equipped with an ORTEC EDS system, at 15kV accelerating voltage and 1nA of beam current . The following standards were used: albite (Na), diopside (Mg), Fe_2O_3 (Fe), Ai_2O_3 (Al), SiO_2 (Si), K-feldspar (K), apatite (Ca), TiO_2 (Ti), MnO_2 (Mn). Mineral diagnostics were proved by X-ray powder methods on Siemens D-500 diffractometer with Cu K_α-radiation. IR spectroscopy was carried out on UR-20 analyser on pressed monomineral powder tablets in the range: diopside 1500-400; amphibole 3800-400; phlogopite 4000-400 cm^{-1}.

Mineralogy

Diopside, $CaMgSi_2O_6$, is an important calcium magnesium silicate, which is a major mineral in the diopside marbles (Fig. 3) found in the valley of the Modi-Khola river. Generally, in the marble strata from Unit II of the Greater Himalayan metamorphites, three morphological types of diopsides occur:

1. Large prismatic crystals, forming nests at the crossings of Type II pegmatite with the marble stratum. Usually the crystals reach 6-7 cm in length and 1-2 cm in width, but in some cases crystals up to 10 cm are found. They associate with carbonate minerals, quartz and needle-like small tourmaline crystals.

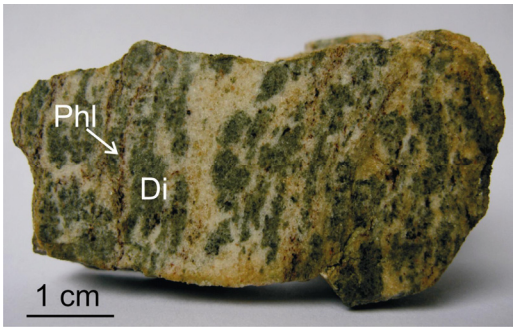

Fig. 3. Diopside-phlogopite marble from the Modi-Khola valley. (Di) diopside; (Phl) phlogopite

2. Irregular crystals and grains forming nests, lenses and veinlets in the marbles. They are more abundant in the zones near the pegmatites, sometimes representing ~50% of the rock volume. These diopside aggregations have massive and granular texture, forming dark green layers, which sometimes alternate with phlogopite thin layers (Fig. 3). The crystal size is generally up to 0.5 cm.

3. The smallest (up to 0.2 cm), almost colorless and sporadic crystals are located in the distal parts of the embedding marble horizons.

The habit of the single pyroxene crystals is prismatic, reflecting the monoclinic structure of infinite cation polyhedral chains along the *c*-axis. Crystals observed on SEM are shaped by *a*{100} and *b*{010}, while *c*{001} form is often presented by multiple-tip terminations (Fig. 4A). The crystal edges are rounded and the crystal faces are striated. Irregular and skeletal shape is also typical (Fig. 4B).

The first pyroxene structure determined was that of diopside (Warren & Bragg 1928). This work established that the essential feature of all pyroxene structures is the linkage of SiO_4 tetrahedra by sharing two out of four corners to form continuous chains of $(SiO_3)n$. The repeat distance along the chain is approximately 5.2 Å, defining the *c*-parameter of the unit cell. The chains are linked laterally by cations (Ca, Na, Mg, Fe), whose positions are labeled *M*1 and *M*2. The *M*1 positions lie principally between the apices of SiO_3 chains, whereas *M*2 lie between their bases. While the *M*1 positions are occupied by relatively smaller Mg atoms in nearly regular octahedral coordination of oxygen atoms, the *M*2 in diopside are preferably occupied by Ca (Na) in irregular, eight-fold coordination.

Diopside belongs to the group of Ca-clinopyroxenes with space group C2/*c* according to the approved nomenclature of pyroxenes (Morimoto 1989). The chemical composition of the studied diopside crystals varies according to the position towards the pegmatite source. Two chemical types of diopside crystals can be distinguished:

1. Green diopsides from the proximal zone, with 8.36-9.94 wt.% FeO and 11.39-12.47 wt.% MgO. Representative analyses are quoted in Table 1 (analyses 1-3). Following the procedure, recommended by Morimoto (1989), the mean composition of these pyroxenes is $(Ca_{0.98}Mg_{0.02})_{1.00}(Mg_{0.65}Fe_{0.30}Al_{0.05})_{1.00}Si_{2.00}O_6$; showing average $Mg/(Mg+Fe^{2+})$ ratio of 0.69. The increased Fe-content defines the pyroxene as ferroan-diopside.

2. White crystals from the distal zones, with 2.69-5.74 wt.% FeO, and MgO in the range 14.92-20.38 wt.%. Representative analyses are shown in Table 1 (analyses 4-6). Their mean crystal - chemical formula can be

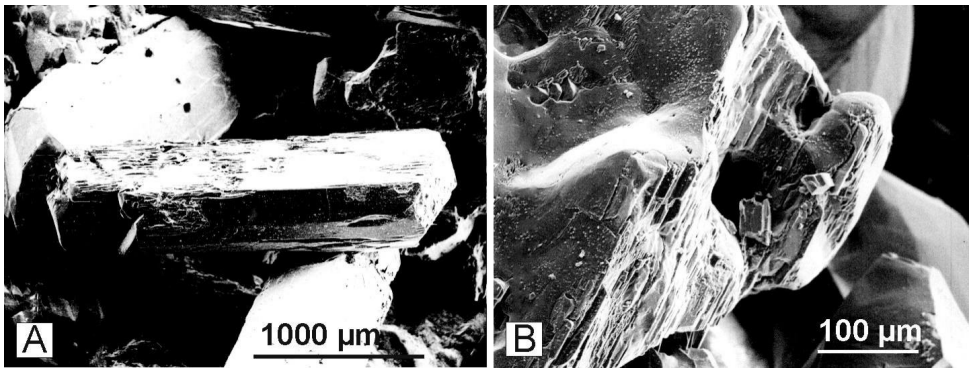

Fig. 4. Morphology of diopside crystals extracted from the Modi-Khola marbles. (A) prismatic well-shaped crystal; (B) irregular skeletal crystal with rounded edges

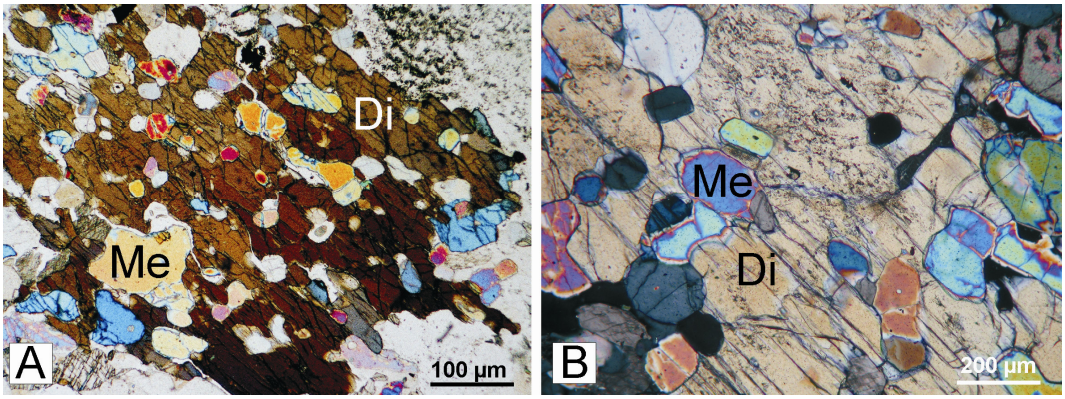

Fig. 5. Diopside–scapolite relationships in cross polarized light. A) skeletal diopside crystal containing scapolite euhedral grains; B) scapolite crystals with different orientation in diopside. Abbreviations: (Di) diopside; (Me) meionite

written as follows:
$(Ca_{0.92}Mg_{0.08})_{1.00}(Mg_{0.88}Fe_{0.12})_{1.00}(Si_{1.94}Al_{0.06})_{2.00}O_6$.
The average $Mg/(Mg+Fe^{2+})$ value for these diopsides is 0.89.

The Fe-content of the pyroxenes influences some differences in their physical constants. The specific gravity measured for the green crystals is 3.43. Members of the diopside - hedenbergite solid solution have 3.22-3.38 (quoted for diopsides) and 3.50-3.56 (for hedenbergite) according to Deer et al. (1997). The higher gravity value for the studied pyroxene is due to the presence of the relatively heavier ferroan ions in the *M*1 position of the pyroxene structure.

Diopside is monoclinic, biaxial (+). In thin sections the subhedral to anhedral pyroxene grains are transparent, colorless, non-pleochroic, sometimes with very weak pleochroism in plane polarized light. Birefringence is 0.032. The measured values for the angle between the optical axes 2V are in the range 60-63°, and are more typical for the hedenbergites compared with those stated in Deer et al. (1997).

The unit-cell parameters obtained by the XRD-study are: *a* 9.749(3); *b* 8.921(1); *c* 5.249(7) Å; *β* 105.836(8)°, showing slight differences with those quoted for the pure diopside (Deer et al. 1997).

The following trace elements were determined in diopside: Be 20; V<10; Cr 10; Ba 1000; Zn 30; Ga 20; Ag 0.3; Sn 10; Pb 10; Zr<100; Co<10; Ni<10; Ti 100; Mn 3000; Li<30 ppm.

The main absorption lines in the IR spectra of the diopside are presented in Table 2.

Scapolite, $(Na,Ca)_4[Al_3Si_9O_{24}](Cl,CO_3)$, actually represents a series of sodium chloride-rich mariallite and calcium carbonate-rich analog, meionite.

In the marbles from the Modi-Khola valley, scapolite is very often found in association with diopside. The crystals of this framework alumosilicate can reach 1 mm in length, but are usually smaller. It was observed in the pyroxene lenses and layers, intimately intergrown with diopside. Its euhedral crystals are developed in the voids formed within the skeletal pyroxene crystals (Fig. 5A, B).

The tetragonal prismatic crystals are white to colorless. The morphology determined by SEM, shows that crystals are shaped mostly by *a*{100}, *m*{110}, *o*{111} and *c*{001} (Fig. 6), although complete crystals are relatively rare. The shapes of the individual grains are distorted, edges and faces are uneven.

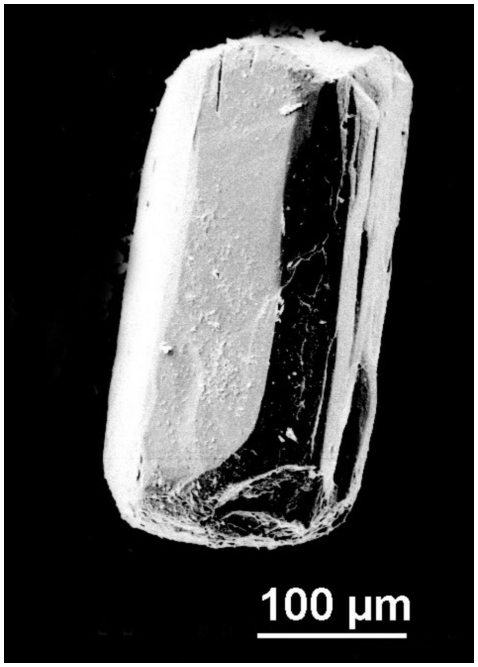

Fig. 6. Scapolite morphology

According to the chemical composition the mineral is determined as *meionite* member of the marrialite-meionite series. The meionite content is ~80 mol% Me, CaO is 18.44 wt.%, while the Na_2O is only 3.2 wt.%. FeO content barely reaches 0.14 wt.%.

The unit-cell parameters obtained by the XRD-study are: *a* 12.181(1); *c* 7.571(7) Å, in good accordance with those quoted for meionites from Slyudyanka in Teertstra & Sheriff (1996). The larger Ca-ions are accommodated in an irregular eightfold coordinated *M* position of the scapolite structure (Sheriff et al. 2000), influencing a trend of increase in the cell-parameters along the marialite-meionite series (e.g. *a* 12.06(1); *c* 7.551(5) Å - marialite and *a* 12.20(1); *c* 7.576(5) Å - meionite) (Teertstra & Sheriff 1996).

Actinolite, $Ca_2(MgFe^{2+})_5Si_8O_{22}(OH)_2$, is also an important silicate, formed as a retrograde mineral after diopside. It is presented as *c*-elongated long-prismatic crystals concentrated in lenses and zones around the pegmatite bodies of Type II. In such massive aggregations the mineral represents almost 90% of the rock, together with some large flake-like phlogopite crystals, late carbonates and quartz (Fig. 7).

Microscopic observation on amphibole crystals in plane polarized light reveals euhedral to subhedral prismatic crystals and rhombic sections. The latter showing perfect [110] cleavage at 124°. In thin sections they are colorless to pale green, non-pleochroic, sometimes with weak pleochroism. Birefringence is 0.025. The studied amphibole is biaxial (-), with 2V 75°, typical for actinolite (Deer et al. 1997). Specific gravity measured is 3.125.

The components in the general chemical formula of amphibole $AB_2C_5T_8O_{22}(OH)_2$ could be grouped as follows: A – K, Na; B – Ca, Na; C – Fe, Mg, Ti, Mn; T – Si, Al, Ti (Leake et al. 1997, 2003). The group of calcic amphiboles with actinolite-tremolite composition is defined as monoclinic members in which $Ca_B>1.5$, $Ca_A<0.5$, $(Na+K)_A<0.5$, and $Mg/(Mg+Fe)>0.5$ and Si is in the range 7.5-8 *apfu* and space group *C2/m*.

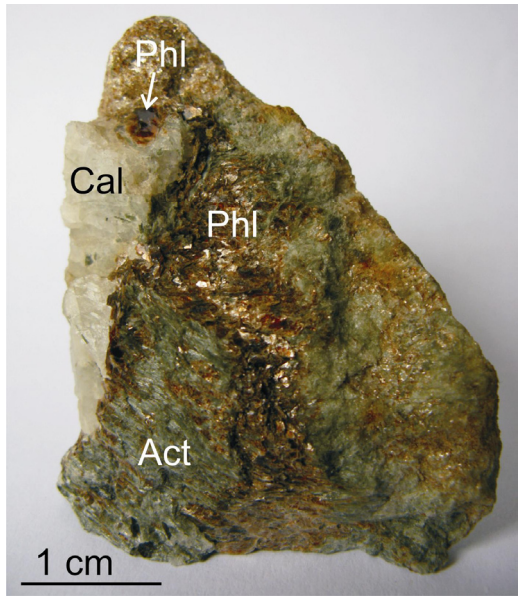

Fig. 7. Actinolite-phlogopite association. (Act) actinolite; (Phl) phlogopite

The MgO content in the studied amphiboles is 15.41-16.68 wt.%, and the FeO ranging 13.16-13.54 wt.% (Table 1). The following chemical formula can be assigned: $Ca_{1.92}Mg_{3.48}Fe_{1.60}Al_{0.14}Si_{7.86}O_{22}(OH)_2$. The mean $Mg/(Mg+Fe^{2+})$ ratio is exactly the same as in the replaced pyroxene - 0.69, defining the mineral as actinolite member of the tremolite - ferro-actinolite series. The replacement of Si by Al is relatively small being up to 0.2 *apfu* Al. The upper limit for the Si-Al tetrahedral replacement is 0.5 *apfu* Al, which is arbitrarily defined by nomenclature (Leake et al. 1997, 2003).

The unit-cell parameters obtained by XRD study are: *a* 9.843(7); *b* 18.049(4); *c* 5.285(8) Å; β 104.877(1)°. The amphibole structure consists of two principal elements, a double chain of corner-sharing tetrahedral and a strip of edge-sharing octahedral, each of which extend in *c*-direction. Both the tetrahedrally coordinated site and the tetrahedra themselves are denoted by *T*, and the octahedrally coordinated sites and the octahedra are denoted by *M*. Two topologically distinct types of tetrahdera are designated *T*1 and *T*2, and three types of octahedra are designated *M*1, *M*2, *M*3, while the junction of the strip of octahedra and the chain of tetrahedral is *M*4 (Hawthorne et al. 2007).

The following trace elements were determined in amphibole: Be 3; V 20; Cr 20; Ba<600; Zn 3000; Ga 20; Ag 0.6; Sn 20; Pb 3; Zr 200; Co 10; Ni 10; Ti 300; Mn 3000; Li 60 ppm.

Table 1. *Representative EPMA analyses of diopside, actinolite, phlogopite and titanite in the calc-silicate rocks from the Modi-Khola valley*

Oxide, wt%	green diopside			white diopside			amphibole		phlogopite		titanite
	O = 6						O = 23		O = 12		O = 5
	1	2	3	4	5	6	7	8	9	10	11
Na_2O	0.00	0.00	0.15	0.00	0.08	0.05	0.01	0.00	0.03	0.00	0.00
MgO	12.47	11.39	11.64	14.92	20.38	17.64	16.68	15.92	16.50	24.01	0.35
Al_2O_3	0.00	1.97	2.29	0.70	1.25	1.83	1.17	0.71	17.07	16.64	4.58
SiO_2	52.77	52.40	52.79	55.67	52.32	52.02	54.64	54.61	40.52	36.30	30.83
K_2O	0.00	0.31	0.27	0.00	0.09	0.05	0.00	0.02	9.87	9.48	0.53
CaO	24.63	23.32	23.65	25.81	22.39	22.64	12.45	12.61	0.00	0.00	28.87
TiO_2	0.00	0.00	0.00	0.01	0.02	0.00	0.02	0.01	0.66	0.83	34.37
MnO	0.00	0.00	0.00	0.20	0.01	0.11	n.d	n.d	0.00	0.18	0.07
FeO	9.94	8.87	9.83	2.69	3.45	5.74	13.54	13.16	10.46	7.46	0.41
total	99.81	98.26	100.62	100.00	99.99	100.08	98.51	97.04	95.11	94.90	100.01
Na	0.00	0.00	0.01	0.00	0.01	0.00	0.00	0.00	0.00	0.00	0.00
Mg	0.70	0.65	0.65	0.82	1.09	0.96	3.53	3.43	1.84	2.58	0.02
Al	0.00	0.09	0.10	0.03	0.05	0.08	0.20	0.12	1.50	1.42	0.17
Si	1.99	2.01	1.97	2.05	1.88	1.90	7.76	7.90	3.03	2.62	0.98
K	0.00	0.02	0.01	0.00	0.00	0.00	0.00	0.00	0.94	0.87	0.02
Ca	1.00	0.96	0.95	1.02	0.86	0.88	1.90	1.95	0.00	0.00	0.98
Ti	0.00	0.00	0.00	0.00	0.00	0.00	0.00	0.00	0.04	0.05	0.82
Mn	0.00	0.00	0.00	0.01	0.00	0.00	n.d	n.d	0.00	0.01	0.00
Fe	0.31	0.28	0.31	0.08	0.10	0.17	1.61	1.59	0.65	0.45	0.01
Mg/ (Mg+Fe)	0.69	0.70	0.68	0.91	0.91	0.85	0.69	0.68	0.74	0.85	-

Table 2. *Infrared absorption bands in the spectra of diopside, actinolite and phlogopite from the Modi-Khola valley*

Diopside					Actinolite		Phlogopite
1	2	3	4	5	6	7	8
							3710
					3675	3675	3660
					3662		3555
						3450	3440
					1632	1635	1635
					1105	1102	
1070	1070	1070	1067	1070	1065	1050	1090
					994	995	995
960	960	966	960	965	950	950	958
917	917	920	920	920	920	920	915
860	853	860	878	865			810
					757	756	770
					730	730	725
674	671	674	674	672	685	685	690
					664	662	658
632		633	633	642	642	642	642
					545	542	
507	507	515	510	508	507	507	
460	458	462	460	464	463	460	465
							450
410	407	409	410	408	415	412	410

(1, 2) small white diopside crystals; (3) pale green diopside prismatic crystal; (4, 5) green skeletal diopside crystals; (6, 7) actinolite long-prismatic crystals; (8) phlogopite flake-like crystals

The bands of absorpition of infrared light of actinolite are presented in Table 2.

Phlogopite, $K(MgFe^{2+})_3AlSi_3O_{10}(OH)_2$, is abundant in the calc-silicate rocks from the Modi-Khola valley. It forms monomineral zones in the marble horizons. These phlogopite marbles show clear cleavage in accordance with the equal orientation of the mica crystals in the fine strata. It occurs also in small layers in association with diopside (Fig. 3). The grain dimensions vary between 0.1 mm and 0.5 mm and grain boundaries may be either perfectly pseudo-hexagonal or more often irregular in outline. Larger up to 1 cm, orange to brown, flake-like crystals are often observed in the amphibole lenses found near the pegmatite bodies, where these two minerals are intimately connected. Phlogopite is overgrowing actinolite crystals (Fig. 7).

Morphology of phlogopite observed with SEM shows thin platy, layered crystals (Fig. 8A) and aggregates of flake-like crystals (Fig. 8B).

In thin sections, under microscope phlogopite is observed as bronze brown to pale orange crystals with birefringenece of 0.040. Weak pleochroism is observed. It is monoclinic, biaxial (-), although it behaves almost as monoaxial with very small angle between the optical axes 2V 15°. Cleavage on (001) is perfect. Specific gravity measured is 3.25.

Phlogopite structure is basic for 1M trioctahedral micas. Rayner (1974) refined this structure using single-crystal neutron diffrac-

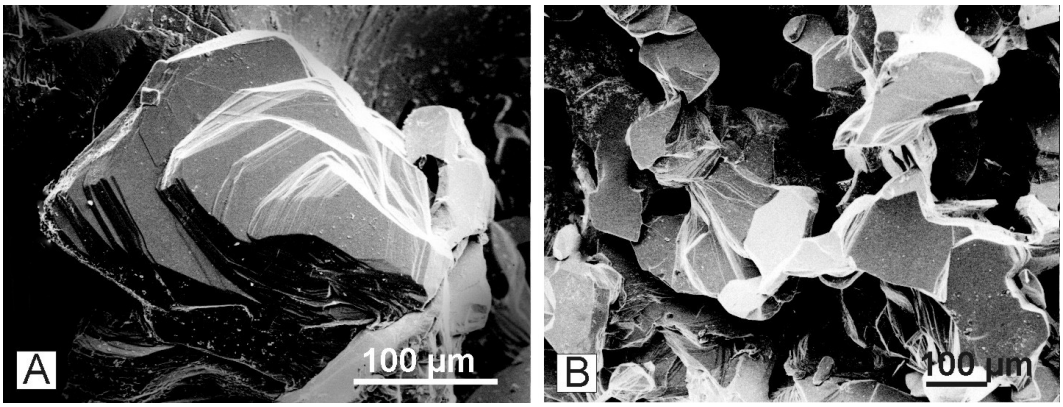

Fig. 8. Phlogopite morphology. A) single crystal; B) aggregate of flake-like crystals

tion reflection data, which permitted precise determination of H atom position. The unit-cell parameters of the studied phlogopite, obtained by XRD study *a* 5.31(7); *b* 9.20(4); *c* 10.31(8) Å; β 99.9(1)° are almost equivalent with those quoted for phlogopite in Fleet et al. (2003).

According to it's chemical composition and considering the Nomenclature of the Micas (Rieder et al. 1998) the mineral is determined as a Mg-member of the annite-phlogopite solid solution, belonging to the group of trioctahedral true micas (K>0.5 *apfu*; octahedral cations > 2.5 *apfu*). EPMA analyses show 16.50-24.01 wt.% MgO, ~ 9.68 wt.% K_2O and up to 0.83 wt.% TiO_2. The FeO range of 7.46-10.46 wt.% classifies the mineral as ferroan-phlogopite (Table 1, analyses 9-10). Fe^{2+} substitutes for Mg^{2+}. The mean chemical composition can be present by the formula: $K_{0.94}Mg_{2.22}Fe_{0.55}Ti_{0.04}Mn_{0.01}Al_{1.28}(Si_{2.82}Al_{0.18})_{3.00}O_{10}(OH)_2$.

The main absorption lines in the infrared spectra of phlogopite are presented in Table 2. Infrared spectroscopy, applied on phlogopite, shows various bands in the OH-streching region (3800-3200 cm^{-1}), which are typical for micas and other phyllosilicates and are associated with local differences in the cation environment of the OH group (Fleet et al 2003). Amongst trioctahedral micas, as in the studied phlogopite the primary OH-stretching mode is at about 3710 cm^{-1} (Table 2). The occurring three broad bands in the 3440-3620 cm^{-1} region result from the association of the OH group with vacancies in the octahedral layer, typical especially for biotites and phlogopites with high Fe content (Wunder & Melzer 2002; Fleet et al. 2003). Considering Jenkins (1989) we may assume that the 995, 958, and 465 cm^{-1} vibrations are influenced by Si, the 810 and 770 cm^{-1} vibrations by Al, the 915 and 725 cm^{-1} vibrations by Al and Si. It is shown also that the 690 and 495 cm^{-1} vibrations are strongly linked to Mg and not just Si. The 658 cm^{-1} band in phlogopite is attributed to an in-plane Al-O vibration rather than an Al-O-Si vibration. The increased Fe content in the phlogopites leads to the complexity of spectra in the 3400 – 3800 cm^{-1} region and shift of the dominant bands to lower wave numbers (Vedder 1964).

The following trace elements were determined in phlogopite: Be 10; V 30; Cr 30; Ba 1000; Zn 600; Ga 20; Ag 0.1; Sn 10; Pb 3; Zr 500; Co 10; Ni 10; Ti 6000; Mn 1000; Li 600 ppm.

Titanite, $CaTiSiO_5$, is a minor mineral, occurring as small 0.1-0.2 mm well-shaped crystals in the carbonate matrix of the diopside marbles (Fig. 9). The crystal faces are presented by *a*{100}, *c*{001} and *n*{111}, although SEM observation on titanite grains reveal traces of growth in limited space, uneven faces, irregular edges (Fig. 10). The representative chemical analysis of the studied

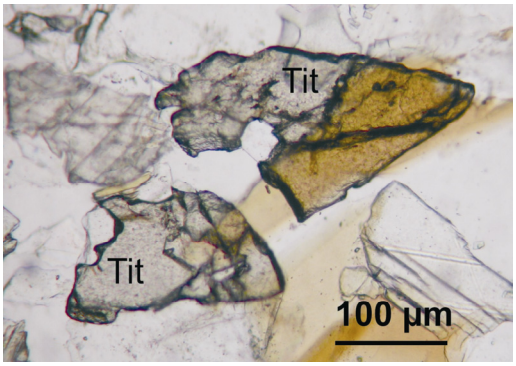

Fig. 9. Titanite crystal in carbonate matrix, together with some phlogopite, plane polarized light

mineral is quoted in Table 1 (analyse 11). The following chemical formula can be assigned: $Ca_{0.98}(Ti_{0.83}Al_{0.17}Fe_{0.01})Si_{1.01}O_5$.

Troilite, FeS, is a common minor mineral in the diopside marbles. The bronze, platy crystals have tabular habit and irregular hexagonal morphology (Fig. 11). Its chemical composition $Fe_{0.99}S$ is nearly stoichiometric defining the mineral as troilite. Pyrrhotite shows naturally strong magnetism, although the studied mineral is antiferrimagnetic, because of the almost equal charge of the Fe^{2+} and S^{2-}. Such pyrrhotites show hexagonal symmetry, while those having ferromagnetic properties are mainly monoclinic (Morimoto 1975; Kontny et al. 2000).

Tourmaline, is very common mineral in the Greater Himalayan metamorphites. In the diopside marbles and calc-silicate rocks it occurs as small, up to 1 mm long, needle-like crystals, marking the pegmatite boundaries. It associates with long-prismatic diopside crystals, quartz and later carbonates. Under microscope tourmaline is green, to brown-green, with characteristic zonal structure of the single crystals (Fig. 12).

Mineral relationships

Diopside skeletal crystals accommodate scapolite euhedral grains within the formed voids (Fig. 5). This means, that either these two minerals are formed together in the process of regional metamorphism of the marble layers or meionite is formed earlier, before diopside, considering the well-shaped crystals and euhedral scapolite grains. The structure of scapolite is very similar to that of feldspars, belonging to framework silicates. The studied diopside marbles contain feldspar grains, seen under microscope and we tend to assume that scapolite crystals are formed after anortite considering also the chemical composition of these two minerals.

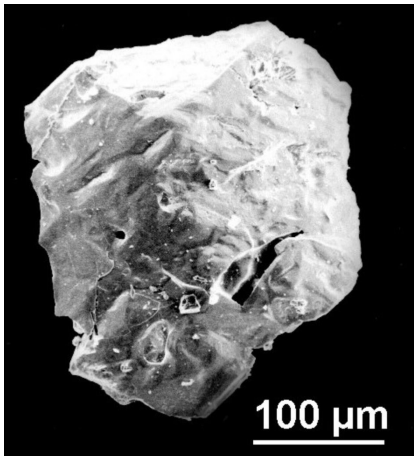

Fig. 10. SEM image of titanite morphology

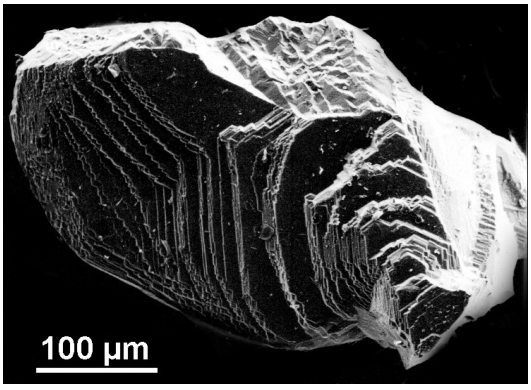

Fig. 11. SEM image of troilite morphology

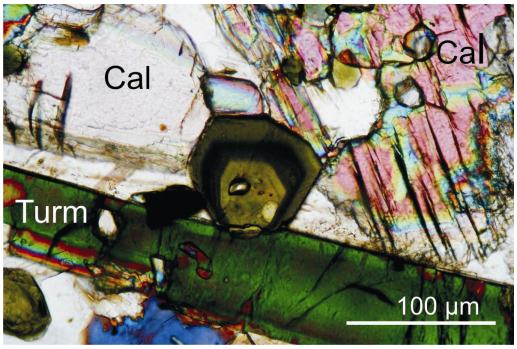

Fig. 12. Zonal tourmaline crystal, cross polarized light

In the retrogressive phase actinolite is formed after diopside. Oriented, irregular relics of diopside, which behave as one crystal are often observed in amphibole crystals (Fig. 13). Diopside is partly to almost fully transformed in the process of retrograde alteration, following the reaction:

$5Ca(MgFe)Si_2O_6 + 3CO_2 + H_2O =$
diopside
$Ca_2(MgFe)_5Si_8O_{22}(OH)_2 + 3CaCO_3 + 2SiO_2$
actinolite calcite quartz

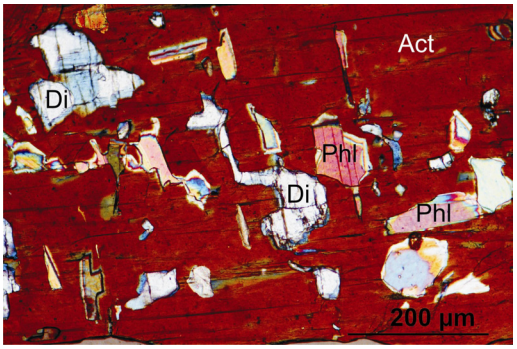

Fig. 13. Oriented diopside relics, behaving as one crystal in actinolite, cross polarized light. (Di) diopside; (Act) actinolite; (Phl) phlogopite

The pyroxene-amphibole transition is based on the similarities in the structures of these two minerals: the chains of SiO_4 tetrahedra in the diopside structure doubles in the structure of actinolite.

On the other hand, actinolite itself becomes unstable under decreasing temperature and is easily replaced by phlogopite. Evidences for that transition are the oriented phlogopite crystals overgrowing actinolite, seen under microscope (Fig. 14).

Phlogopite is formed not only after actinolite, considering the mica amount in the rocks, where phlogopite forms monomineral layers in the marbles from the upper levels of the section through the Modi-Khola river. A probable process of formation is the transformation of diopside and microcline to phlogopite with the active participation of aqueous solutions:

$3CaMgSi_2O_6 + KAlSi_3O_8 + H_2O + 3CO_2 =$
diopside microcline
$KMg_3AlSi_3O_{10}(OH)_2 + 3CaCO_3 + 6SiO_2$
phlogopite calcite quartz

The *P-T* conditions of formation of calc-silicates and marbles from Unit II are determined to be 500-580°C and 3-5 kbar (Schneider & Masch 1993).

Conclusions

1. The diopside and phlogopite marbles are a major rock type in the Greater Himalayan metamorphite sequence, representing the informal Unit II defined by many authors (Bordet et al. 1971; Le Fort 1975, 1981; Colchen et al. 1986; Pêcher 1989; Guillot et al. 1995; Searle & Godin 2003).
2. The calc-silicate rocks are formed in the process of overall prograde metamorphism in the Great Himalaya. The intrusion of pegmatite bodies, cross-cutting the marble strata leads to processes of recrystallization and consolidation of the silicates in the interaction zone.

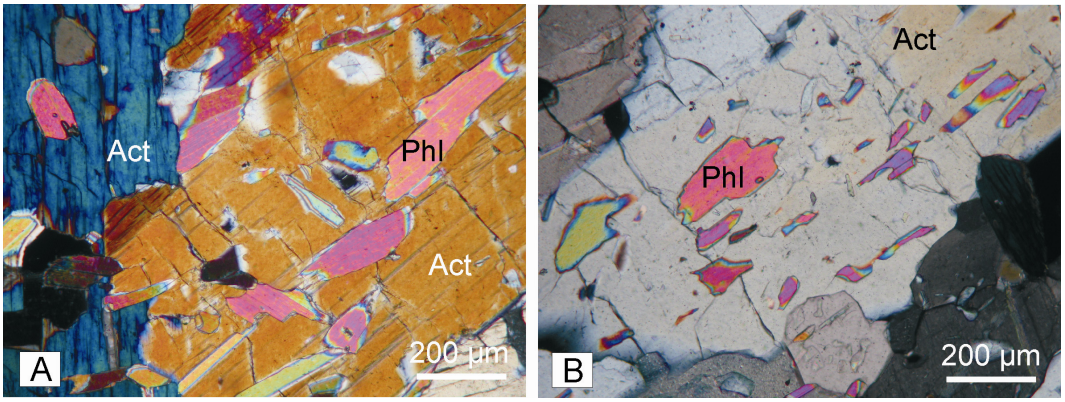

Fig. 14. Actinolite crystals replaced by oriented phlogopite flakes. (Act) actinolite; (Phl) phlogopite

3. Meionite is formed together with diopside or shortly before it. Diopside is altered by actinolite in the retrogressive stage, and actinolite is replaced by phlogopite. The pyroxene-amphibole-mica transition is determined by transformations based on the similarities in the crystal structures.

4. The minerals in the studied calc-silicate rocks are formed in a Mg-enriched environment, where Fe^{2+} also plays an important role. All silicate minerals have increased iron content and in addition pyrrhotite is formed in the late hydrothermal stage. The presence of tourmaline indicates enhanced boron activity.

References

Bordet P, Colchen M, Krummenacher D, Le Fort P, Mouterde R, Remy M (1971) *Recherche géologiques dans l'Himalaya du Népal: Région de la Thakkhola.* Paris, CNRS, p 279

Colchen M, Le Fort P, Pêcher A (1986) *Annapurna-Manaslu-Ganesh Himal*. Paris, CNRS, p 136

Deer WA, Howie RA, Zussman J (1997) *Rock-forming minerals, Single-chain silicates*, vol. 2A, second edition, The Geological Society, London, 198-293

Deer WA, Howie RA, Zussman J (1997) *Rock-forming minerals. Double-chain silicates*, vol. 2B, second edition, The Geological Society, London, 135-232

Dhital MR, Thapa PB, Ando H (2002) Geology of the inner Lesser Himalaya between Kusma and Syangja in western Nepal. *Bulletin of the Department of Geology, Tribhuvan University, Kathmandu, Nepal*, **9,** 1–60

Fleet ME (2003) *Rock-forming minerals. Sheet silicates: Micas*, vol. 3A, second edition, The Geological Society, London, 325-521

Ganguly J, Dasgupta S, Cheng W, Neogi S (2000) Exhumation history of a section of the Sikkim Himalayas, India: Records in the metamorphic mineral equilibria and compositional zoning of garnet. *Earth and Planetary Science Letters*, **183**, 471–486

Garzanti E (1999) Stratigraphy and sedimentary history of the Nepal Tethys Himalaya passive margin. *Journal of Asian Earth Sciences*, **17**, 805–827

Godin L (2003) Structural evolution of the Tethyan sedimentary sequence in the Annapurna area, central Nepal Himalaya. *Journal of Asian Earth Sciences*, **22**, 307-328

Godin, L, Gleeson T, Searle MP, Ullrich TD, Parrish RR (2006) Locking of southward extrusion in favour of rapid crustal-scale buckling of the Greater Himalayan sequence, Nar valley, Central Nepal. In: Law RD, Searle MP, Godin L (editors) *Channel flow, ductile extrusion and exhumation in Continental collision zones*. Geological Society, London, Special Publication, **268**, 269-292

Guillot S, Le Fort P, Pêcher A, Barman MR, Aprahamian J (1995) Contact metamorphism

and depth of emplacement of the Manaslu granite (central Nepal): implications for Himalayan orogenesis. *Tectonophysics*, **241**, 99–119

Jenkins DM (1989) Empirical study of the infrared lattice vibrations (1100–350 cm^{-1}) of phlogopite. *Physics and Chemistry of Minerals*, **16**, 408-414

Hawthorne FC, Oberti R, Ventura GD, Mottana A (editors) (2007) Amphiboles: Crystal Chemistry, Occurence, and Health Issues. *Reviews in Mineralogy and Geochemistry*, **67**, 545 p.

Hodges KV, Parish RR, Searle MP (1996) Tectonic evolution of the central Annapurna range, Nepalese Himalaya. *Tectonics*, **15**, 1264-1291

Kohn MJ, Wieland M, Parkinson CD, Upreti BN (2004) Miocene faulting at plate tectonic velocity in the Himalaya of central Nepal. *Earth and Planetary Science Letters*, **228,** 299–310

Kontny A, de Wall H, Sharp TG, Pósfai M (2000) Mineralogy and magnetic behavior of pyrrhotite from a 260°C section at the KTB drilling site, Germany. *American Mineralogist*, **85**, 1416-1427

Leake BE et al. (1997) Nomenclature of amphiboles: Report of the Subcommittee on amphiboles of the International Mineralogical Association, CNMM. *The Canadian Mineralogist,* **35**, 219-246

Leake BE et al. (2003) Nomenclature of amphiboles: Additions and revisions to the International Mineralogical Association's 1997 Recommendations. *The Canadian Mineralogist,* **41**, 1355-1362

Le Fort P (1975) Himalayas: The collided range. Present knowledge of the continental arc. *American Journal of Science* **275-a,** 1–44

Le Fort P (1981) Manaslu leucogranite: A collision signature of the Himalaya - a model for its genesis and emplacement. *Journal of Geophysical Research*, **86**, 545–568

Martin AJ, DeCelles PG, Gehrels GE, Patchett PJ, Isachsen C (2005) Isotopic and structural constraints on the location of the Main Central thrust in the Annapurna Range, central Nepal Himalaya. *Geological Society of America Bulletin*, **117,** 926–944

Myrow PM, Hughes NC, Paulsen TS, Williams IS, Parcha SK, Thompson KR, Bowring SA, Peng SC, Ahluwalia AD (2003) Integrated tectonostratigraphic analysis of the Himalaya and implications for its tectonic reconstruction. *Earth and Planetary Science Letters*, **212**, 433–441

Morimoto N (1989) Nomenclature of pyroxenes. Subcommittee on pyroxenes of the International Mineralogical Association, CNMMN. *The Canadian Mineralogist*, **27**, 143-156

Morimoto N, Gyobu A, Mykaiyama H, Izawa E (1975) Crystallography and stability of pyrrhotites. *Economic Geology*, **70**, 824-833

Murphy MA, Yin A (2003) Structural evolution and sequence of thrusting in the Tethyan fold-thrust belt and Indus-Yalu suture zone, Southwest Tibet. *Geological Society of America Bulletin*, **115**, 1, 21–34

Pêcher A (1989) The metamorphism in the central Himalaya. *Journal of Metamorphic Geology*, **7**, 31–41

Rayner JH (1974) The crystal structure of phlogopite by neutron diffraction. *Mineralogical Magazine*, **39**, 850-856

Richards A, Argles T, Harris NBW, Parrish RR, Ahmad T, Darbyshire F, Dragantis E (2005) Himalayan architecture constrained by isotopic tracers from clastic sediments. *Earth and Planetary Science Letters*, **236**, 773–796

Rieder M, Cavazzini G, D'Yakonov YS, Frank-Kamenetskii VA, Gottardi G, Guggenheim S, Koval PV, Mueller G, Neiva AMR, Radoslovich EW, Robert J-L, Sassi FP, Takeda H, Weiss Z, Wones D (1998) Nomenclature of the Micas. *The Canadian Mineralogist*, **36**, 3, 905-912

Schneider C, Masch L (1993) The metamorphism of Tibetan series from Manangarea, Marsyandi valley, central Nepal. In: Treilar PJ, Searle MP (Eds.) *Himalayan tectonics, Geological Society of London Special Publication*, **74**, 357-374

Searle MP, Godin L (2003) The South Tibetan detachment and the Manaslu Leucogranite: a structural reinterpretation and restoration of the Annapurna-Manaslu Himalaya, Nepal. *Journal of Geology*, **111,** 505–523

Searle MP, Simpson RL, Law RD, Parrish RR, Waters DJ (2003) The structural geometry, metamorphic and magmatic evolution of the Everest Massif, High Himalaya of Nepal-South Tibet. *Journal of the Geological Society of London*, **160,** 3, 345–366

Sheriff BL, Sokolova EV, Kabalov YK, Jenkins DM, Kunath-Fandrei G, Goetz S, Jaeger G, Schneider J (2000) Meionite: Rietveld structure refinement, 29Si MAS and 27Al SATRAS NMR Spectroscopy, and comments on marialite-meionite series. *The Canadian Mineralogist*, **38**, 1201-1213

Stephenson BJ, Waters DJ, Searle MP (2000) Inverted metamorphism and the Main Central Thrust: field relations and thermobarometric

constraints from the Kishtwar Window, NW Indian Himalaya. *Journal of Metamorphic Geology*, **18**, 5, 571–590

Teertstra DK, Sheriff BL (1996) Scapolite cell-parameters trend along the solid-solution series. *American Mineralogist*, **81**, 169-180

Tischendorf G, Förster H-J, Gottesmann B (2001) Minor- and trace-element composition of trioctahedral micas: A review. *Mineralogical Magazine*, **65**, 2, 249-276

Vedder W (1964) Correlations between the infrared spectrum and chemical composition of mica. *American Mineralogist*, **49**, 736-768.

Warren BE, Bragg WL (1928) The structure of diopside, $CaMg(SiO_3)_2$. *Zeitschrift fűr Kristallographie*, **69**, 168-193

Wunder B, Melzer S (2002) Interlayer vacancy characterization of synthetic phlogopitic micas by IR spectroscopy. *European Journal of Mineralogy*, **14,** 1129-1138

Accepted June 11, 2008
Приета на 11.06.2008 г.